

1 Re-submitted to: *Chemosphere* (CHEM 22722, revised as a Technical Note)

2 Date: 19 August 2011

3  
4 **Investigation of the role of biopolymer clusters in MBR membrane fouling**  
5 **using flash freezing and environmental scanning electron microscopy**

6  
7 **Xiao-mao Wang,<sup>a</sup> Fei-yun Sun<sup>a,b</sup> and Xiao-yan Li<sup>a\*</sup>**

8 <sup>a</sup> Environmental Engineering Research Centre, Department of Civil Engineering,  
9 The University of Hong Kong, Pokfulam Road, Hong Kong, China

10 <sup>b</sup> Harbin Institute of Technology, Shenzhen Graduate School, Shenzhen 518055, China

11 (\*Corresponding author: phone: 852-28592659; fax: 852-28595337; email: xlia@hkucc.hku.hk)

12  
13 **Abstract**

14 The technique that employs flash freezing and environmental scanning electron microscopy  
15 (ESEM) was utilised for detailed investigation of the fouling materials in a membrane  
16 bioreactor (MBR). The method involves the flash freezing of a wet sample in liquid nitrogen  
17 for 10 s to preserve its structure for direct ESEM observation with a high image resolution.  
18 ESEM images show that the sludge cake formed by simple filtration of the MBR bulk sludge  
19 has a highly porous, sponge-like structure with a fairly low resistance. However, the fouling  
20 layer attached to the membrane surface contains a thin gel-layer under the main body of the  
21 sponge-like sludge cake, which is similar to that formed by filtration of a dispersion of  
22 biopolymer clusters (BPCs). It is apparent that BPCs tend to accumulate on the membrane  
23 surface, and the gel layer is largely responsible for the high filtration resistance of the cake  
24 layer on the fouled membranes.

26 **Keywords:** Biological wastewater treatment; Biopolymer clusters (BPCs); Environmental  
27 scanning electron microscope (ESEM); Flash freezing; Fouling layer; Membrane bioreactor  
28 (MBR).

29

## 30 **1. Introduction**

31

32 Membrane bioreactors (MBRs) are increasingly applied to biological wastewater treatment  
33 owing to their ensured solids–water separation and excellent effluent quality for reuse  
34 purposes (Judd, 2006; Yang et al., 2006). However, membrane fouling, which is caused  
35 primarily by foulant deposition on the membrane surface, remains far and away the major  
36 limitation to the cost-effectiveness of MBRs for large-scale applications (Asatekin et al.,  
37 2007). Numerous efforts have been devoted to obtaining a fundamental understanding of the  
38 membrane fouling mechanisms (Le-Clech et al., 2006) that is essential for the development  
39 of effective fouling control technologies. It is generally believed that the deposition of a  
40 fouling (cake or gel) layer on the membrane surface is the major form of membrane fouling  
41 during MBR operation (Chu and Li, 2005; Wang et al., 2007). A number of foulants have  
42 been identified that would be responsible for the fouling layer formation, including biomass  
43 sludge (Defrance et al., 2000), the extracellular polymeric substances (EPS) in sludge  
44 (Nagaoka et al., 1996; Drews et al., 2006), soluble microbial products (SMP) and other forms  
45 of organic matter in the liquid phase (Rosenberger et al., 2006; Liang et al., 2007). Therefore,  
46 the roles played by different foulants, and their interactions in membrane fouling during  
47 MBR operation, however, still require investigation.

48 The supernatant of the MBR sludge mixture has been found to have a consistently  
49 higher organic concentration than the effluent from the MBR (Shin and Kang, 2003; Holakoo  
50 et al., 2006). It is therefore believed that the organic materials in the sludge suspension

51 contribute significantly to the development of membrane fouling (Judd, 2006; Ng et al., 2006;  
52 Rosenberger et al., 2006; Liang et al., 2007). Studies have further indicated that biopolymer  
53 clusters (BPCs) are one of the primary foulants in the MBR system (Wang et al., 2007; Sun et  
54 al., 2008; Wang and Li, 2008). BPCs are formed by the clustering of SMP and loose EPS in  
55 the sludge cake. BPCs are much larger in size than SMP, and they differ from bacterial flocs  
56 in that they are composed of few microorganisms. It has become clear that the difference in  
57 organic concentration between the supernatant of the MBR sludge and its permeate effluent is  
58 due to the retention of BPCs by membrane filtration. Meanwhile, BPC formation and  
59 accumulation in turn would cause serious membrane fouling during MBR operation (Sun et  
60 al., 2010b). However, the role played by BPCs in fouling layer formation and its effect on  
61 membrane permeability remain to be determined.

62 Detailed examination of the fouling layer structure on the membrane surface is greatly  
63 needed for better understanding of the MBR fouling mechanisms and the interactions of  
64 different foulants during the fouling process. Such examination is also extremely important to  
65 the development of more effective membrane fouling alleviation strategies. For example, a  
66 further increase in shear intensity may not be effective for membrane fouling reduction if the  
67 top layers of the sludge cake contribute little to its filtration resistance. Similarly, the  
68 commonly applied back-flushing technique (Wu et al., 2008) may have a low degree of  
69 effectiveness if BPCs accumulate mainly at the bottom of the sludge cake and cover the  
70 membrane surface. Chemical cleaning from the permeate side may be more effective in this  
71 case (Chang et al., 2002). The advanced microscopic techniques used to date to examine  
72 foulants and fouling layers, including scanning electron microscopy (SEM), confocal laser  
73 scanning microscopy (CLSM) and atomic force microscopy (AFM), are unsatisfactory.  
74 Conventional SEM examination requires samples to undergo dehydration followed by sputter  
75 coating (Miura et al., 2007), whereas samples for CLSM must be stained using specific

76 fluorescent dyes before observation (Chu and Li, 2005; Hwang et al., 2008). As the foulants  
77 are highly hydrated, porous and soft, the SEM sample pretreatment steps can cause the  
78 significant deformation, or even collapse, of the structure and morphology of the foulants and  
79 fouling layers (Fig. 1a and 1b). AFM scan requests little sample treatment and the images can  
80 have a fairly high resolution. This, however, is the case only for rather hard surfaces. The  
81 AFM images of the fouling layers on membrane are usually blurry owing to the soft nature of  
82 the foulants (Huisman et al., 2000; Martinez et al., 2000; Song et al., 2004). Moreover, AFM  
83 as a surface scanning technique is apparently not suitable for examination of thick sludge  
84 cake layers, as is also the case for CLSM. In the latter, the free dyes may remain in the cake,  
85 and the fouling layers may produce false images that are difficult to discern.

86 Environmental SEM (ESEM, or, more generally, variable-pressure SEM) is another  
87 technique employed for the direct observation of highly hydrated samples including fouling  
88 layers (Le-Clech et al., 2007), but requires no dehydration and sputter coating steps.  
89 Omission of the dehydration step allows preservation of the sample contents and structure.  
90 However, the maximum magnification possible for ESEM observations at room temperature  
91 could be restricted, being determined by the limitation of the useful specimen distance, which  
92 may lead to a loss of specimen details. Thus, most ESEM images of the fouling layers on the  
93 membrane surface look rather blurry (Le-Clech et al., 2007). The other problem for ESEM is  
94 the specimen dehydration resulted from water evaporation at room temperature in the low-  
95 pressure (one to several hundred Pa) specimen chamber, which often leads to significant  
96 sample shrinkage and structure deformation. This problem is more severe for highly hydrated  
97 specimens, as is the case for the gel and/or cake layers responsible for membrane fouling (Fig.  
98 1c and 1d). However, both the magnification and resolution can be significantly improved  
99 and the specimen dehydration can be greatly minimized if the specimen is cryogenically

100 fixed and maintained frozen on the cold stage during ESEM examinations (Santiwong et al.,  
101 2009; Wang and Waite, 2009).

102 In this study, the flash freezing technique with liquid nitrogen coupled with ESEM  
103 examination was adopted for the first time to examine the shape and structure of the MBR  
104 foulants and fouling layers. In view of the known role of BPCs in membrane fouling, focuses  
105 were placed on the characterisation of the fouling properties of BPCs and determination of  
106 the spatial distribution of BPCs in the sludge cake layer. The findings would provide  
107 important insight into the mechanisms of membrane fouling in MBRs.

108

## 109 **2. Materials and methods**

110

### 111 *2.1. Sludge and BPC samples*

112 The sludge and BPC samples were obtained from a submerged MBR that had been in  
113 stable operation for more than 4 yr (Sun et al., 2010b). A 0.2 m<sup>2</sup> polyethylene hollow-fibre  
114 membrane module was immersed in the cuboid plexiglass reactor, which had a working  
115 volume of 5 L. The feed to the reactor was a mixture of synthetic wastewater and actual  
116 domestic sewage. The synthetic wastewater was prepared according to the basic recipe of  
117 AEESP (2001) to supply about 90% of the organic load in the influent, and the actual sewage  
118 was collected from a local wastewater treatment plant (Stanley Sewage Treatment Works,  
119 Hong Kong). The influent had a total organic carbon (TOC) concentration of around 220 mg  
120 L<sup>-1</sup>, and the concentration of the mixed liquor suspended solids (MLSS) in the MBR was  
121 maintained at about 5.1 g L<sup>-1</sup>. Continuous aeration was applied under the membrane module,  
122 and an intermittent filtration mode was applied with a switch on/off ratio of 18 min/2 min for  
123 membrane fouling minimisation. The sludge and hydraulic retention times were 20 d and 6 h,  
124 respectively, which corresponded to a food-to-microorganism ratio of 0.125 g TOC g<sup>-1</sup> MLSS

125  $\text{d}^{-1}$  and a filtration flux of  $0.1 \text{ m}^3 \text{ m}^{-2} \text{ d}^{-1}$ . The reactors were operated at room temperature (22-  
126 25 °C), and the water temperature was 20-22 °C. The TOC concentration in the liquid  
127 samples was determined with a TOC analyser (IL550 TOC-TN Analyzer, Lachat).

128 The bulk sludge (BS) was obtained directly from the MBR sludge mixture. Special  
129 attention was paid to the cake sludge (CS) that gradually built up on the membrane during  
130 MBR operation. When the membrane was severely fouled, as indicated by a trans-membrane  
131 pressure (TMP) of about 80 kPa, the CS deposited on the membrane was thoroughly removed  
132 from the membrane fibres and re-suspended in water until to a sludge concentration of about  
133  $5 \text{ g MLSS L}^{-1}$ . In addition to the CS mixture, the CS suspension was further separated by  
134 sedimentation at 4 °C for 12 h into the CS supernatant and settled CS solids. The CS  
135 supernatant is known to contain a high concentration of organic solutes deemed to be BPCs  
136 (Wang et al., 2007; Lin et al., 2009). A filterability test was carried out on the four samples,  
137 i.e., the BS mixture, CS suspension, settled CS solids and CS supernatant, to determine their  
138 specific resistance to filtration. The filtration test was conducted using microfiltration (MF)  
139 membrane filters ( $0.4 \mu\text{m}$ , Osmosis) following the method that has been used by Wisniewski  
140 and Grasmick (1998) and Wang et al. (2007). More importantly, the sludge or gel layers  
141 deposited on the MF filters were then processed for the subsequent ESEM examination.

142

## 143 *2.2. ESEM observation*

144 A flash freezing technique was adopted to preserve the sludge or gel layers. This  
145 method has been previously employed (Santiwong et al., 2008; Wang and Waite, 2008) to  
146 examine the structure of highly porous gel layers. As stated above, resolution of the ESEM  
147 images can also be greatly enhanced if the wet samples are fixed by freezing. Prior to ESEM  
148 observation, each membrane filter with a wet cake or gel layer was carefully cut into  $10 \times 5$   
149 mm slices. The filter with the sample was then dipped in a liquid nitrogen bath for about 10 s.

150 After the simple flash freezing, the sample was frozen into a fragile solid that could easily be  
151 snapped to display a nearly flat edge or cutaway section. The sample specimen was then  
152 placed under an ESEM (S-3400N, variable-pressure SEM, Hitachi) on a cold stage (-25 °C,  
153 MK2-cool stage, Deben). The sample was not conductive, and a back-scattered electron (BSE)  
154 signal was used for imaging. In actuality, use of BSE signal is necessary to allow a high  
155 resolution of the ESEM images. Moreover, the fouled membrane fibres were also cut off  
156 from the MBR, and the morphology and micro-structure of the CS formed on the membrane  
157 surface were examined using the same flash freezing-ESEM technique.

158

### 159 **3. Results and discussion**

160

#### 161 *3.1 Sludge and BPC layers*

162 The volume and structure of the wet sludge deposition on the filter surface were well  
163 preserved by the flash freezing method using liquid nitrogen, thus allowing the porous  
164 structure of the deposition layer to be examined directly via ESEM. A highly porous structure  
165 with many large pores (Fig. 2) was observed for the cake layer formed through filtration of  
166 the BS suspension from the MBR. The size of these pores was apparently of the same  
167 magnitude as the sludge flocs, i.e., tens of  $\mu\text{m}$ . The packing of the sludge flocs was found to  
168 form a sponge-like structure conducive to water passage. Such distinct ESEM images  
169 showing the micro-structural details of the sludge cake would not be obtained with the  
170 conventional SEM (Fig. 1a and 1b), which requires a dehydration step. In comparison to the  
171 ESEM photos of the sludge cake taken at room temperature without prior flash freezing (Fig.  
172 1c and 1d), the quality of the images in Fig. 2 is largely improved in terms of both resolution  
173 and structure preservation.

174 Filtration of the MBR BS suspension through the MF filter was actually fairly easy.  
175 The filtration test showed the BS mixture to have a mass-based specific resistance of only 3.4  
176  $\times 10^{11}$  m kg<sup>-1</sup> (Fig. 3), which is comparable to that reported by Buyukkamaci (2004) and  
177 Wang et al. (2007). The degree of filtration resistance remained low when a thick BS cake  
178 layer was formed on the MF filter. It can thus be deduced that the membrane module in a  
179 MBR would not become seriously fouled if only such a sludge cake was formed on the  
180 membrane.

181 The CS mixture, in contrast, was rather difficult to filter through the MF filter. The  
182 CS removed from the fouled membrane in the MBR displayed a much greater specific  
183 filtration resistance, i.e., at a level of around  $1.4 \times 10^{14}$  m kg<sup>-1</sup> (Fig. 3). The CS had a high  
184 organic content, about 20 mg TOC g<sup>-1</sup> SS, much higher than that of the MBR BS, which was  
185 around 1 mg TOC g<sup>-1</sup> SS. The settled CS solids underwent an order of magnitude reduction in  
186 specific filtration resistance (around  $2.1 \times 10^{12}$  m kg<sup>-1</sup>) compared to the original CS mixture.  
187 The organic content of the CS was dissolved into the supernatant to give it a TOC  
188 concentration of more than 40 mg L<sup>-1</sup>. The CS supernatant had a much lower filterability, as  
189 it formed a gel layer on the MF filter with a specific resistance (around  $1.7 \times 10^{14}$  m kg<sup>-1</sup>)  
190 similar to that of the CS mixture. The organic solutes in the supernatant, which are classified  
191 as BPCs, have been recognised as an important foulant in MBR systems (Wang et al., 2007;  
192 Sun et al., 2008). BPCs play an essential role in sludge deposition and cake layer formation  
193 on the membrane surface during MBR operation, and they are also primarily responsible for  
194 the great filtration resistance of the CS (Wang and Li, 2008; Lin et al., 2009; Sun et al., 2011a,  
195 2011b).

196 The flash freezing treatment allows direct examination of BPCs on the filter surface  
197 (Fig. 4). The BPC layer showed a gel appearance that is rather different from the BS observed  
198 in Fig. 3. Despite its great filtration resistance, the gel layer formed on the MF filter was only



199 a few  $\mu\text{m}$  in thickness. The dehydration step for common SEM observation would greatly  
200 change the nascent structure and volume of the BPC gel layer. In contrast, as no dehydration  
201 was involved in sample preparation, the BPC layer structure was preserved in the present  
202 study. BPCs are in nature microgels formed by the clustering of SMP, small BPCs and loose  
203 EPS (Wang et al., 2007; Sun et al., 2008). It is apparent that BPCs in the gel layer were inter-  
204 connected (gelated) probably with the aid of multivalent cations (Wang and Waite, 2009). As  
205 a result, the gel layer did not have a sponge-like porous structure. It instead had a very low  
206 porosity at the top surface, which would effectively restrict the passage of water through the  
207 gel layer. Moreover, it is rather difficult to dehydrate a gel, which would further account for  
208 the extremely high specific resistance of the gel layer.

209

### 210 *3.2 Fouling cake layer on the MBR membrane surface*

211 The sludge cake layer on the membrane surface has been investigated in previous  
212 studies. The influences of the operating parameters, such as filtration flux, organic loading  
213 and sludge age, on the MBR fouling process were studied through laboratory experiments  
214 (Wang and Li, 2008). The membrane fouling rate was found to be affected by both the  
215 process variables and the BPC concentration in the sludge mixture. The specific filtration  
216 resistance of the cake layer correlated well with the BPC content in the sludge cake (Wang et  
217 al., 2007). In other words, BPC accumulation appeared to be the primary reason for the high  
218 specific resistance of the sludge fouling layer in MBRs. Because a high hydraulic shear is  
219 normally applied for membrane fouling control during MBR operation, massive sludge  
220 deposition on the membrane is usually prevented if the filtration is below the critical flux  
221 (Cho and Fane, 2002). However, an elevated shear intensity and a lower filtration flux would  
222 favour BPC accumulation in the sludge cake (Wang et al., 2007).

223           The structural detail of the cake sludge formed on the membrane fibre in the MBR  
224 was also revealed by the ESEM images (Fig. 5a and 5b). When the membrane module was  
225 severely fouled, the CS layer could be over 200  $\mu\text{m}$  thick and sometimes cover more than one  
226 fibre. The CS layer attached to the membrane was different from the BS deposition formed  
227 during the filtration test, as indicated by the specific resistance of the former two orders  
228 magnitude higher than that of the latter (Fig. 3). The principal morphology of the CS fouling  
229 layer was similar to that of the BS deposition in terms of the porous structure (porosity and  
230 pore size). However, by a scrutiny of the ESEM images one can find that at the bottom of the  
231 CS layer there was a thin (several  $\mu\text{m}$ ) layer that had a reticulum-like appearance with a mesh  
232 of nodules. The above sponge-like main body formed by biomass sludge could be easily  
233 detached while the thin layer remained attached to the membrane (Fig. 5c and 5d). The thin  
234 layer was composed mainly of organic substances and apparently similar to the BPC gel layer  
235 shown in Fig. 4.

236           The ESEM images also showed the BPC distribution within the CS layer to be non-  
237 uniform, with the BPCs prone to accumulate at the bottom. Compared to CLSM images (Chu  
238 and Li, 2005; Hwang et al., 2008), ESEM images have a higher resolution and show  
239 structural details more clearly. The strong filtration resistance exhibited by the CS is likely  
240 owing to the thin BPC layer, as the top sponge-like structure is fairly permeable. As organic  
241 solutes, BPCs are sticky and flexible and can penetrate with water through the main body of  
242 the porous sludge cake. Over the course of time, however, BPCs would become too large to  
243 pass through the membrane, which could result in their accumulation and thus the formation  
244 of a gel layer on the membrane surface. A small amount of BPC deposition on the membrane  
245 would be sufficient to greatly increase its filtration resistance.

246           It is therefore apparent that BPC coverage of the membrane was brought about  
247 primarily by the retention of organic materials such as SMP during MBR filtration. The

248 accumulation of BPCs in the sludge cake layer would also allow the BPCs to grow in size.  
249 The size of the BPCs in sludge cake has been found to be significantly larger than that in  
250 MBR sludge suspension (Sun et al., 2011b). During MBR operation, in which hydraulic shear  
251 is commonly applied, the BPCs that have not reached the membrane surface, but bind with  
252 the sludge flocs, have a strong chance of being scoured back into the bulk suspension. Thus,  
253 the formation of the thin BPC gel layer on the MBR membrane surface was the result of  
254 long-term operation (e.g., several weeks). Both the ESEM images and the filtration test  
255 showed a thin BPC layer to be sufficient to cause severe membrane fouling. BPC formation  
256 and accumulation within the CS layer are inevitable consequences of the inherent feature of  
257 membrane filtration during MBR operation, i.e., the retention of biomass sludge and organic  
258 foulants, thereby leading to membrane fouling.

259

#### 260 **4. Conclusions**

261 An effective flash freezing-ESEM technique for investigation of fouling layers has been  
262 developed. ESEM images showed the sludge cake formed by simple filtration of the BS to be  
263 highly porous and permeable with a sponge-like structure. Filtration of the BPC dispersion,  
264 however, led to the formation of a gel-layer that was less porous, much less permeable and  
265 displayed a reticulum-like appearance. The CS layer formed was found to contain a thin (< 10  
266  $\mu\text{m}$ ) gel-layer under the main body of the sponge-like sludge cake, which is largely  
267 responsible for the great specific filtration resistance of the cake layer.

268

#### 269 **Acknowledgments**

270 This research was supported by URC funding from the University of Hong Kong,  
271 Special Equipment Grant SEG\_HKU10 from the University Grants Committee (UGC), and  
272 Grants HKU7144/E07 and HKU714811E from the Research Grants Council (RGC) of the

273 Hong Kong SAR Government. The technical assistance of Mr. Keith C. H. Wong is greatly  
274 appreciated.

275

## 276 **References**

277 AEESP, 2001. Environmental Engineering Process Laboratory Manual. Association of  
278 Environmental Engineering and Science Professors, Champaign, IL, USA.

279 Asatekin, A., Kang, S., Elimelech, M., Mayes, A.M., 2007. Anti-fouling ultrafiltration  
280 membranes containing polyacrylonitrile-graft-poly (ethylene oxide) comb copolymer  
281 additives. *J. Membr. Sci.* 298, 136–146.

282 Buyukkamaci, N., 2004. Biological sludge conditioning by Fenton's reagent. *Process*  
283 *Biochem.* 39, 1503–1506.

284 Chang, I.S., Le-Clech, P., Jefferson, B., Judd, S., 2002. Membrane fouling in membrane  
285 bioreactors for wastewater treatment. *J. Environ. Eng.-ASCE.* 128, 1018–1029.

286 Cho, B.D., Fane, A.G., 2002. Fouling transients in nominally sub-critical flux operation of a  
287 membrane bioreactor. *J. Membr. Sci.* 209, 391–403.

288 Chu, H.P., Li, X.Y., 2005. Membrane fouling in a membrane bioreactor (MBR): Sludge cake  
289 formation and fouling characteristics. *Biotechnol. Bioeng.* 90, 323–331.

290 Defrance, L., Jaffrin, M.Y., Gupta, B., Paullier, P., Geaugey, V., 2000. Contribution of  
291 various constituents of activated sludge to membrane bioreactor fouling. *Bioresour.*  
292 *Technol.* 73, 105–112.

293 Drews, A., Lee, C.H., Kraume, M., 2006. Membrane fouling – a review on the role of EPS.  
294 *Desalination* 200, 186–188.

295 Holakoo, L., Nakhla, G., Yanful, E.K., Bassi, A.S., 2006. Chelating properties and molecular  
296 weight distribution of soluble microbial products from an aerobic membrane bioreactor.  
297 *Water Res.* 40, 1531–1538.

298 Huisman, I.H., Pradanos, P., Hernandez, A., 2000. The effect of protein-protein and protein-  
299 membrane interactions on membrane fouling in ultrafiltration. *J. Membr. Sci.* 179, 79–  
300 90.

301 Hwang, B.K., Lee, W.N., Yeon, K.M., Park, P.K., Lee, C.H., Chang, I.S., Drews, A., Kraume,  
302 M., 2008. Correlating TMP increases with microbial characteristics in the bio-cake on  
303 the membrane surface in a membrane bioreactor. *Environ. Sci. Technol.* 42, 3963–3968.

304 Judd, S., 2006. *The MBR Book: Principles and Applications of Membrane Bioreactors in*  
305 *Water and Wastewater Treatment.* Elsevier, Amsterdam, The Netherlands.

306 Le-Clech, P., Chen, V., Fane, T.A.G., 2006. Fouling in membrane bioreactors used in  
307 wastewater treatment. *J. Membr. Sci.* 284, 17–53.

308 Le-Clech, P., Marselina, Y., Ye, Y., Stuetz, R.A., Chen, V., 2007. Visualisation of  
309 polysaccharide fouling on microporous membrane using different characterisation  
310 techniques. *J. Membr. Sci.* 290, 36–45.

311 Liang, S., Liu, C., Song, L., 2007. Soluble microbial products in membrane bioreactor  
312 operation: behaviors, characteristics, and fouling potential. *Water Res.* 41, 95–101.

313 Lin, H.J., Xie, K., Mahendran, B., Bagley, D.M., Leung, K.T., Liss, S.N., Liao, B.Q., 2009.  
314 Sludge properties and their effects on membrane fouling in submerged anaerobic  
315 membrane bioreactors (SAnMBRs), *Water Res.* 43, 3827–3837.

316 Martinez, F., Martin, A., Pradanos, P., Calvo, J.I., Palacio, L., Hernandez, A., 2000. Protein  
317 adsorption and deposition onto microfiltration membranes: The role of solute-solid  
318 interactions. *J. Colloid Interface Sci.* 221, 254–261.

319 Miura, Y., Watanbe, Y., Okabe, S., 2007. Membrane biofouling in pilot-scale membrane  
320 bioreactors (MBRs) treating municipal wastewater: impact of biofilm formation.  
321 *Environ. Sci. Technol.* 41, 632–638.

322 Nagaoka, H., Ueda, S., Miya, A., 1996. Influence of bacterial extracellular polymers on the  
323 membrane separation activated sludge process. *Water Sci. Technol.* 34(9), 165–172.

324 Ng, H.Y., Tan, T.W., Ong, S.L., 2006. Membrane fouling of submerged membrane  
325 bioreactors: Impact of mean cell residence time and the contributing factors. *Environ.*  
326 *Sci. Technol.* 40, 2706–2713.

327 Rosenberger, S., Laabs, C., Lesjean, B., 2006. Impact of colloidal and soluble organic  
328 material on membrane performance in membrane bioreactors for municipal wastewater  
329 treatment. *Water Res.* 40, 710–720.

330 Santiwong, S.R., Guan, J., Waite, T.D., 2008. Effect of ionic strength and pH on hydraulic  
331 properties and structure of accumulating solid assemblages during microfiltration of  
332 montmorillonite suspensions. *J. Colloid Interface Sci.* 317, 214–227.

333 Shin, H.S., Kang, S.T., 2003. Characteristics and fates of soluble microbial products in  
334 ceramic membrane bioreactor at various sludge retention times. *Water Res.* 37, 121–127.

335 Song, W., Ravindran, V., Koel, B.E., Pirbazari, M., 2004. Nanofiltration of natural organic  
336 matter with H<sub>2</sub>O<sub>2</sub>/UV pretreatment: fouling mitigation and membrane surface  
337 characterization. *J. Membr. Sci.* 241, 143–160.

338 Sun, F.Y., Wang, X.M., Li, X.Y., 2008. Visualisation and characterisation of biopolymer  
339 clusters in a submerged membrane bioreactor. *J. Membr. Sci.* 325, 691–697.

340 Sun, F.Y., Wang, X.M., Li, X.Y., 2011a. Effect of biopolymer clusters on the fouling  
341 property of sludge from a membrane bioreactor (MBR) and its control by ozonation.  
342 *Process Biochem.* 46, 162–167.

343 Sun, F.Y., Wang, X.M., Li, X.Y., 2011b. Change in the fouling propensity of sludge in  
344 membrane bioreactors (MBR) in relation to the accumulation of biopolymer clusters.  
345 *Bioresour. Technol.* 102, 4718–4725.

346 Wang, X.M., Li, X.Y., 2008. Accumulation of biopolymer clusters in a submerged membrane  
347 bioreactor and its effect on membrane fouling. *Water Res.* 42, 855–862.

348 Wang, X.M., Li, X.Y., Huang, X., 2007. Membrane fouling in a submerged membrane  
349 bioreactor (SMBR): Characterisation of the sludge cake and its high filtration resistance.  
350 *Sep. Purif. Technol.* 52, 439–445.

351 Wang, X.M., Waite, T.D., 2008. Impact of gel layer formation on colloid retention in  
352 membrane filtration processes. *J. Membr. Sci.* 325, 486–494.

353 Wang, X.M., Waite, T.D., 2009. Role of gelling soluble and colloidal microbial products in  
354 membrane fouling. *Environ. Sci. Technol.* 43, 9341–9347.

355 Wisniewski, C., Grasmick, A., 1998. Floc size distribution in a membrane bioreactor and  
356 consequences for membrane fouling. *Colloids Surf. A* 138, 403–411.

357 Wu, J., Le-Clech, P., Stuetz, R.M., Fane, A.G., Chen, V., 2008. Effect of relaxation and  
358 backwashing conditions on fouling in membrane bioreactor. *J. Membr. Sci.* 324, 26–32.

359 Yang, W.B., Cicek, N., Ilg, J., 2006. State-of-the-art of membrane bioreactors: worldwide  
360 research and commercial applications in North America. *J. Membr. Sci.* 270, 201–211.

361

362

363 **Figure Captions**

364

365 Fig 1. Micrographs of the activated sludge cake layer obtained (a, b) with a conventional  
366 SEM after sample pretreatment involving dehydration and sputter coating and (c, d) with  
367 an ESEM at room temperature without prior flash freezing. The arrow points to the  
368 membrane filter.

369 Fig. 2. ESEM images of (a) the cross-section and (b, c, d) detailed structure of the sludge  
370 cake formed on a MF membrane filter through direct filtration of the suspended bulk  
371 sludge in a MBR. The arrows point to the membrane filter.

372 Fig. 3. Comparison of the specific filtration resistance of the cake and gel layers formed  
373 during filtration of the MBR bulk sludge (AS mixture), the re-suspended MBR cake  
374 sludge (CS mixture), the settled solids of the CS mixture and the CS supernatant after  
375 settling.

376 Fig. 4. ESEM images of a layer of BPCs retained on the MF membrane filter through  
377 filtration of BPC dispersion, with increasing magnification from (a) to (d). The arrows  
378 point to the membrane filter.

379 Fig. 5. ESEM images of (a, b) the sludge cake layer deposited on the membrane module in  
380 the MBR and (c, d) its bottom BPC layer after removal of the main body of the sludge  
381 cake. The arrows point to the hollow-fibre membrane.

382



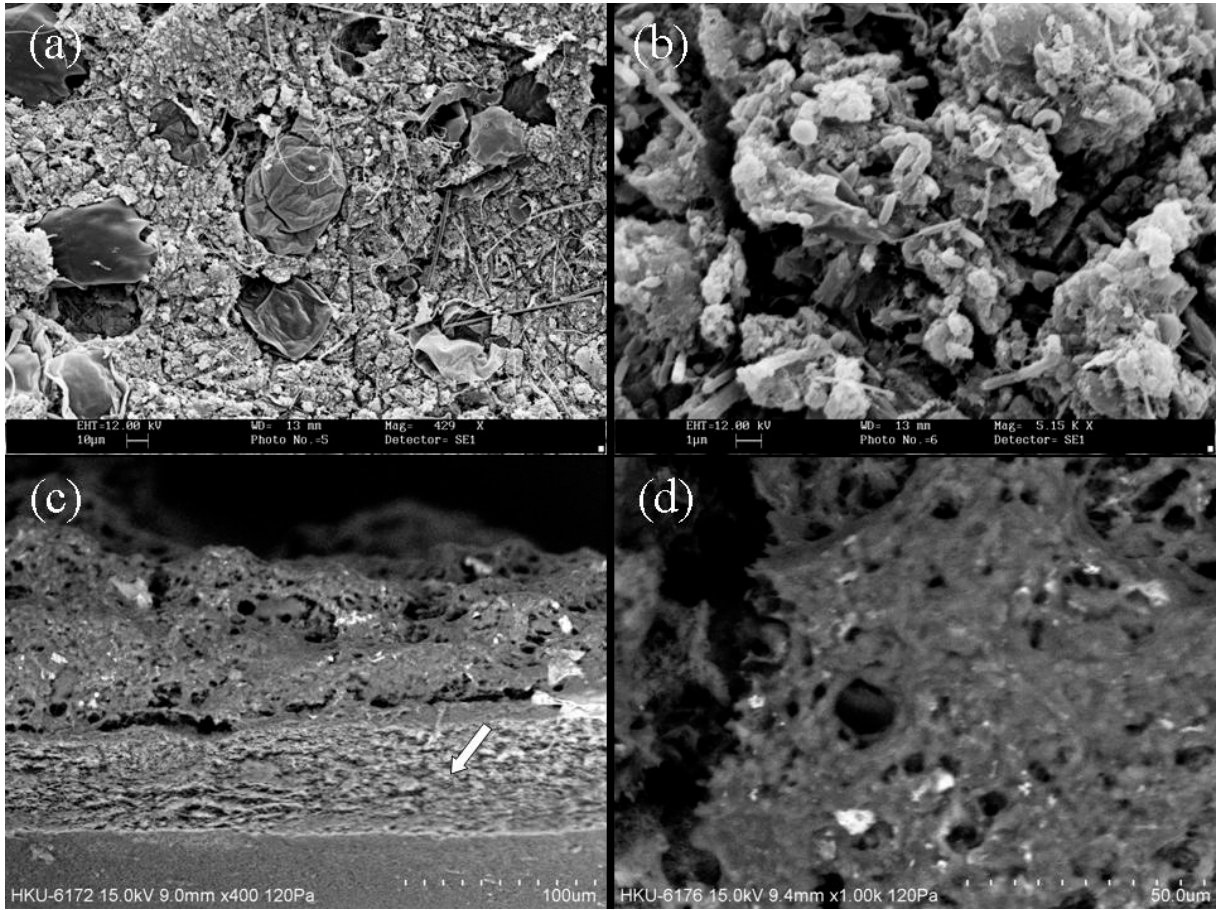


**Fig 1.** Micrographs of the activated sludge cake layer obtained (a, b) with a conventional SEM after sample pretreatment involving dehydration and sputter coating and (c, d) with an ESEM at room temperature without prior flash freezing. The arrow points to the membrane filter.

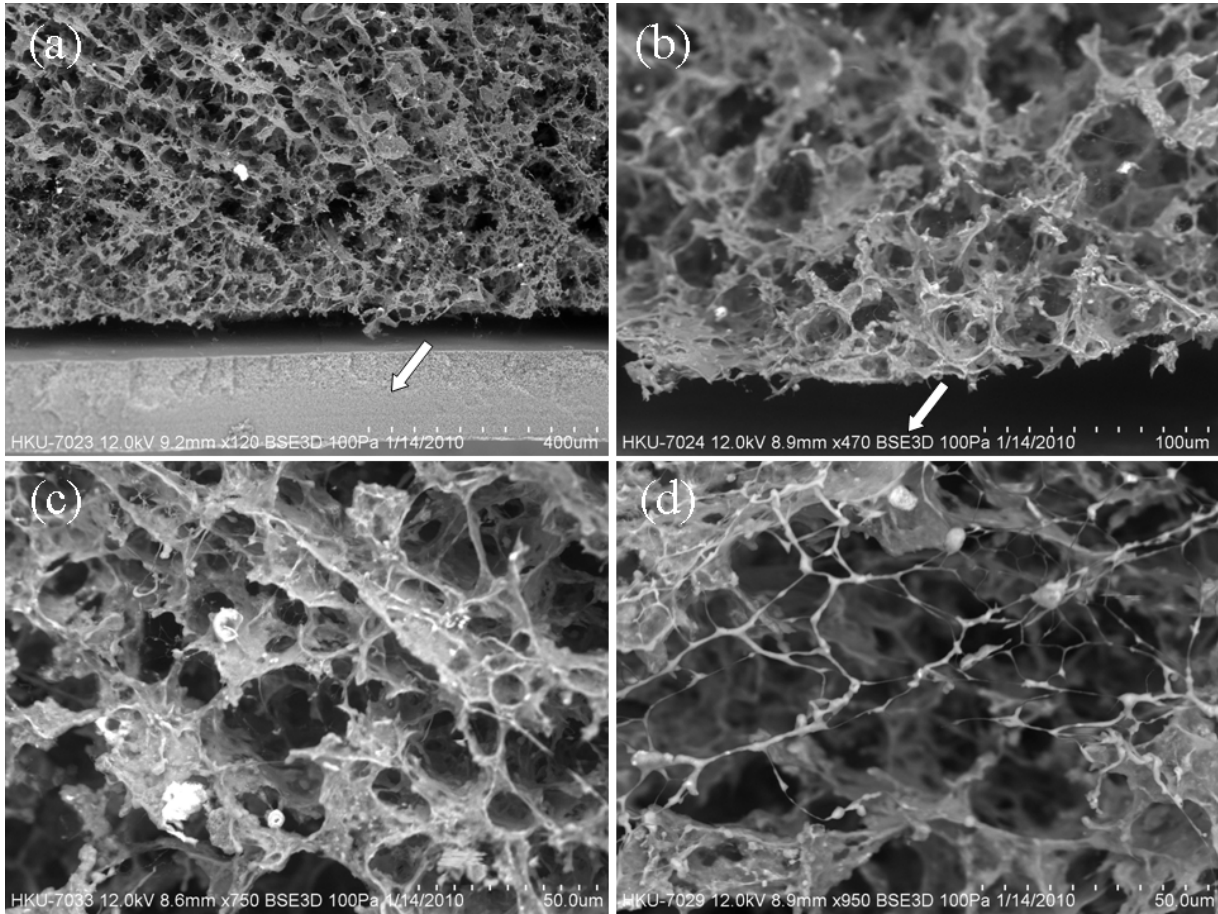


**Fig. 2.** ESEM images of (a) the cross-section and (b,c,d) detailed structure of the sludge cake formed on a MF membrane filter through direct filtration of the suspended bulk sludge from a MBR. The arrows point to the membrane filter.

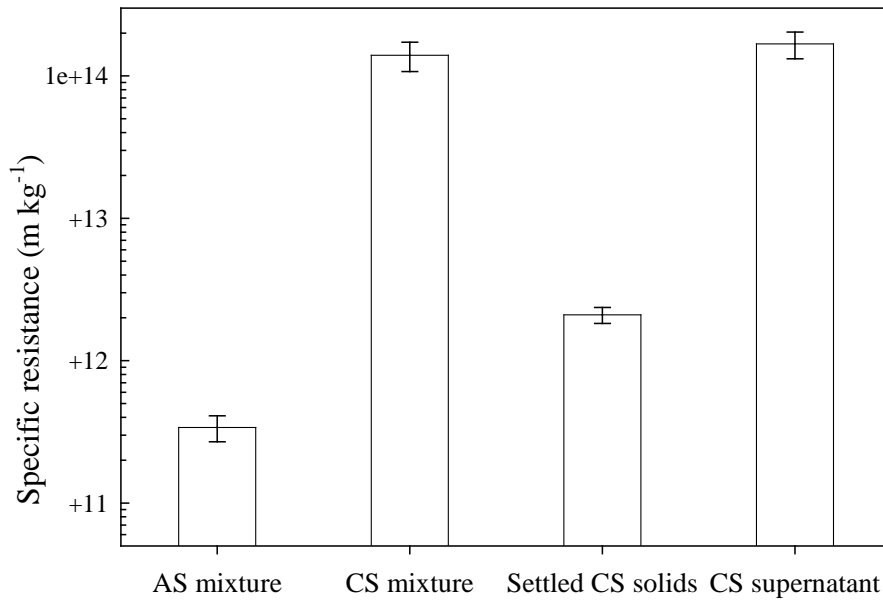


**Fig. 3.** Comparison of the specific filtration resistance of the cake and gel layers formed during filtration of the MBR bulk sludge (AS mixture), the re-suspended MBR cake sludge (CS mixture), the settled solids of the CS mixture and the CS supernatant after settling.

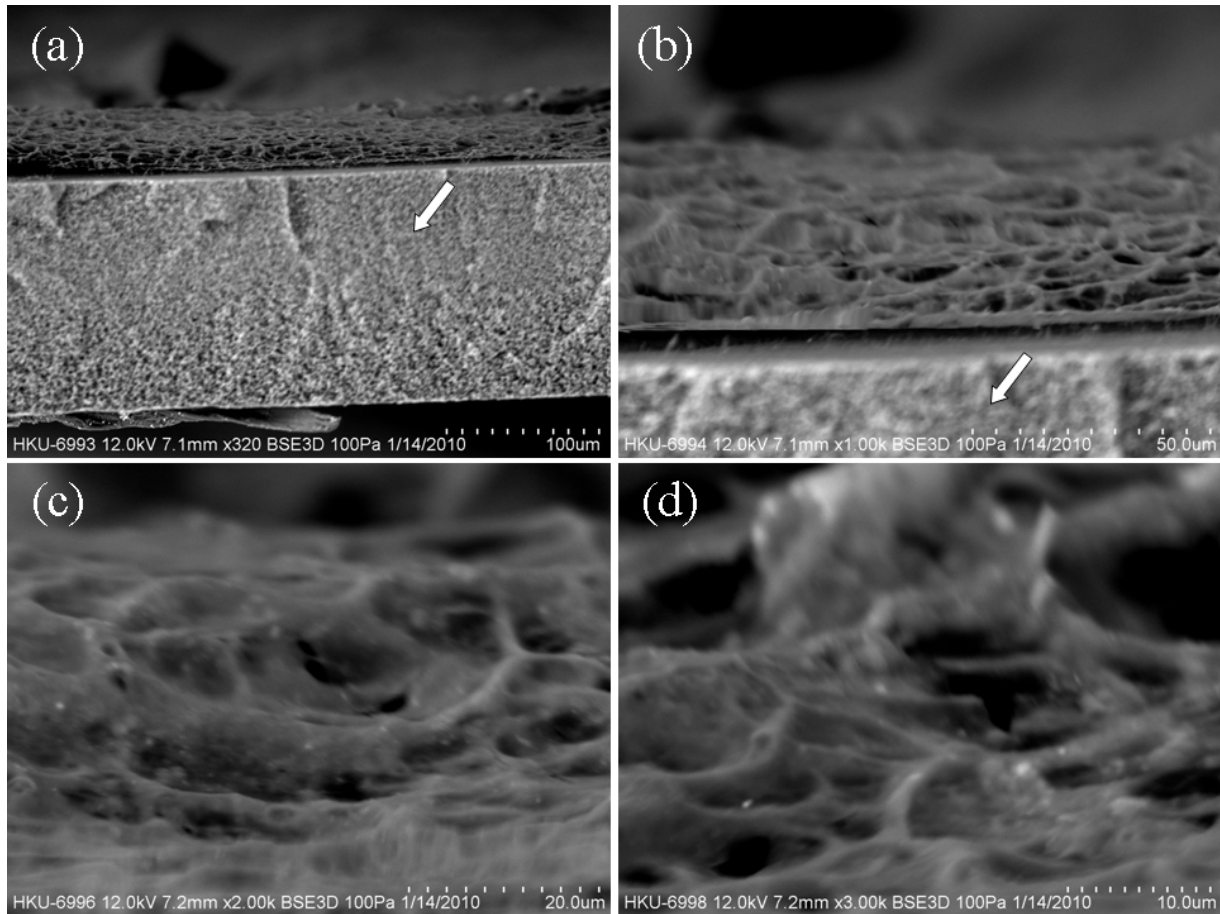


**Fig. 4.** ESEM images of a layer of BPCs retained on the MF membrane filter through filtration of BPC dispersion, with increasing magnification from (a) to (d). The arrows point to the membrane filter.

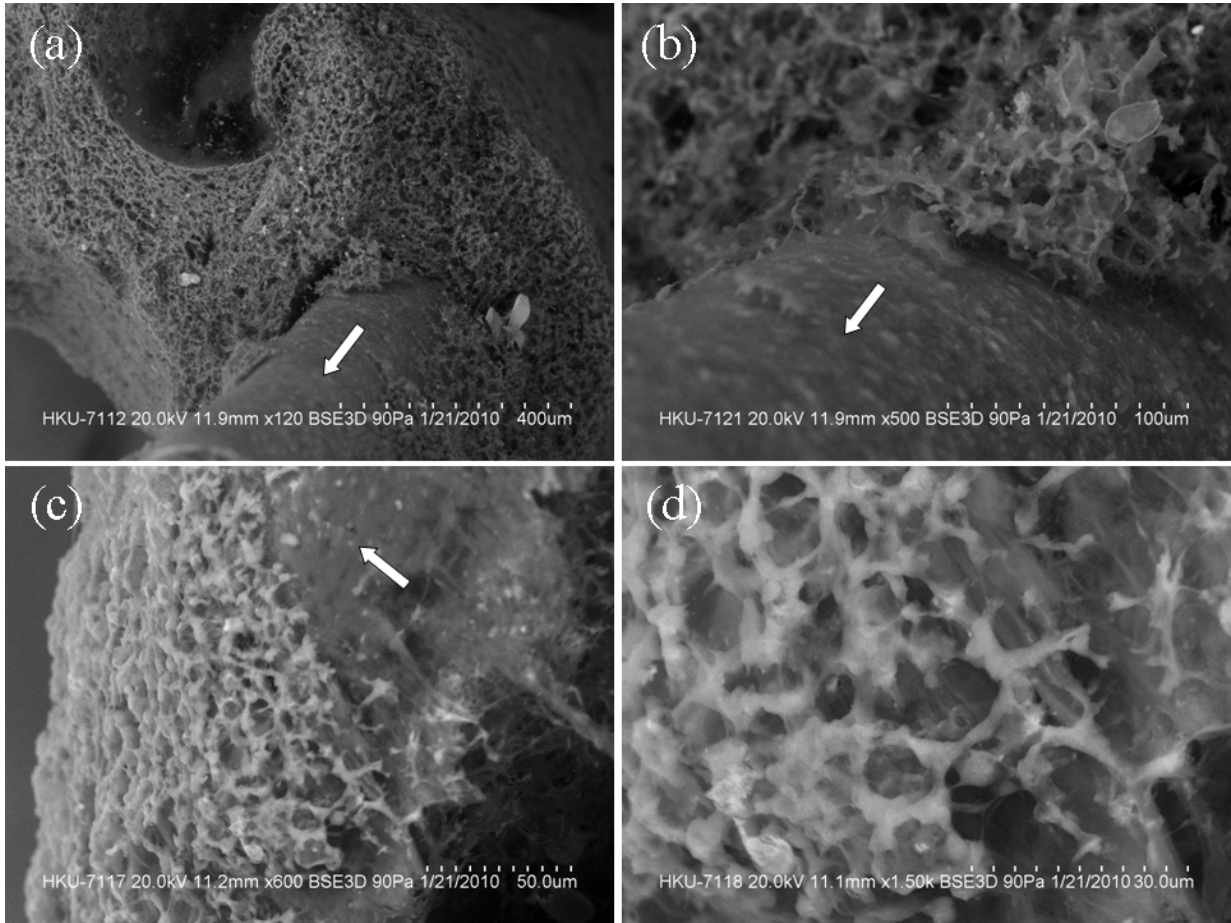


**Fig. 5.** ESEM images of (a,b) the sludge cake layer deposited on the membrane module in the MBR and (c,d) its bottom BPC layer after removal of the main body of the sludge cake. The arrows point to the hollow-fibre membrane.